

# Development of magnesium calcium phosphate biocement for bone regeneration

Junfeng Jia<sup>1</sup>, Huanjun Zhou<sup>1</sup>, Jie Wei<sup>1,\*</sup>, Xin Jiang<sup>1</sup>, Hong Hua<sup>1</sup>,  
Fangping Chen<sup>1</sup>, Shicheng Wei<sup>2</sup>, Jung-Woog Shin<sup>3</sup>  
and Changsheng Liu<sup>1,\*</sup>

<sup>1</sup>Key Laboratory for Ultrafine Materials of Ministry of Education, and Engineering Research Center for Biomedical Materials of Ministry of Education, East China University of Science and Technology, Shanghai 200237, People's Republic of China

<sup>2</sup>Center for Biomedical Materials and Tissue Engineering, Academy for Advanced Inter-disciplinary Studies, Peking University, Beijing 100871, People's Republic of China

<sup>3</sup>Department of Biomedical Engineering, Inje University, First Research Group/BK-21, Gimhae 621-749, Republic of Korea

Magnesium calcium phosphate biocement (MCPB) with rapid-setting characteristics was fabricated by using the mixed powders of magnesium oxide (MgO) and calcium dihydrogen phosphate ( $\text{Ca}(\text{H}_2\text{PO}_4)_2 \cdot \text{H}_2\text{O}$ ). The results revealed that the MCPB hardened after mixing the powders with water for about 7 min, and the compressive strength reached 43 MPa after setting for 1 h, indicating that the MCPB had a short setting time and high initial mechanical strength. After the acid–base reaction of MCPB containing MgO and  $\text{Ca}(\text{H}_2\text{PO}_4)_2 \cdot \text{H}_2\text{O}$  in a molar ratio of 2 : 1, the final hydrated products were  $\text{Mg}_3(\text{PO}_4)_2$  and  $\text{Ca}_3(\text{PO}_4)_2$ . The MCPB was degradable in Tris–HCl solution and the degradation ratio was obviously higher than calcium phosphate biocement (CPB) because of its fast dissolution. The attachment and proliferation of the MG<sub>63</sub> cells on the MCPB were significantly enhanced in comparison with CPB, and the alkaline phosphatase activity of MG<sub>63</sub> cells on the MCPB was significantly higher than on the CPB at 7 and 14 days. The MG<sub>63</sub> cells with normal phenotype spread well on the MCPB surfaces, and were attached in close proximity to the substrate, as seen by scanning electron microscopy (SEM). The results demonstrated that the MCPB had a good ability to support cell attachment, proliferation and differentiation, and exhibited good cytocompatibility.

**Keywords:** magnesium phosphate; calcium phosphate; biocement; degradation; biocompatibility

## 1. INTRODUCTION

Calcium phosphate biocements (CPBs) with excellent biocompatibility and osteoconductivity have been widely studied as bone regeneration materials (Liu *et al.* 2006; Cancedda *et al.* 2007). A typical self-setting CPB, which contained an equimolar mixture of tetracalcium phosphate (TECP) and dicalcium phosphate anhydrous (DCPA), was first reported by Brown & Chow (1986). The TECP/DCPA system CPB set after mixing the powder with water and changed into hydroxyapatite (HA), owing to an acid–base chemical reaction, that had unique *in vivo* properties: slow resorption and replacement by newly formed bone tissue with no loss in volume (Dorozhkin & Eppler 2002; Guo *et al.* 2006, 2009). However, a more rapid

resorption and replacement by new bone tissue is desirable in some clinical cases (Huan & Chang 2007).

Magnesium (Mg) is the fourth most abundant cation in the human body and is naturally found in bone (Staiger *et al.* 2006). It was reported that Mg might be an important factor in the qualitative changes in the bone matrix that determine bone fragility (Rude & Gruber 2004). A previous study showed that Mg indirectly influenced mineral metabolism, for example through activation of alkaline phosphatase (ALP; Arise *et al.* 2008). Another study revealed that the attachment and spreading of cultured human bone-derived cells onto a Mg-coated  $\text{Al}_2\text{O}_3$  bioceramic was significantly enhanced when compared with the uncoated  $\text{Al}_2\text{O}_3$  (Zreiqat *et al.* 2002). Revell *et al.* (2004) noted that a Mg ion-embedded HA coating on titanium alloy significantly improved bone-bonding properties when compared with an ordinary HA coating. Recently, Mg alloys gained more and more attention as a potential

\*Authors for correspondence (biomater2006@yahoo.com.cn; csliu@163.com).

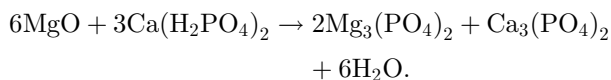
matrix material for biodegradable implants (Staiger *et al.* 2006; Gu *et al.* 2009). Therefore, it is interesting and significant to develop Mg-based biomaterials for bone regeneration.

Mg could decrease the crystallinity and increase the solubility of phosphates after partly substituting calcium (Ca) with Mg (Marchi *et al.* 2007). Brushite biocement incorporating Mg might offer a means of controlling microstructure, strength, composition and resorbability of the cement, and its interaction with host tissues *in vivo* (Hofmann *et al.* 2009). Liu and colleagues prepared magnesium phosphate cement (MPC) consisting of magnesium oxide (MgO) and ammonium dihydrogen phosphate ( $\text{NH}_4\text{H}_2\text{PO}_4$ ) for biomedical applications, which had good biocompatibility after being implanted into cavities in the femoral condyle of rabbits (Liu 1999; Wu *et al.* 2005). Wu *et al.* (2008*a,b*) studied calcium–magnesium phosphate cement (CMPC) by incorporation of MPC into CPC. However, the final hardened product of magnesium ammonium phosphate hexahydrate [ $\text{NH}_4\text{MgPO}_4 \cdot 6\text{H}_2\text{O}$ ] containing the  $\text{NH}_4$  group released  $\text{NH}_3$ , which has some effects on cytocompatibility in a physiological environment. Therefore, a novel Mg-based bone cement of MCPB was designed and developed by using mixed powders of MgO and calcium dihydrogen phosphate ( $\text{Ca}(\text{H}_2\text{PO}_4)_2 \cdot \text{H}_2\text{O}$ ) as raw materials in this study.

## 2. MATERIAL AND METHODS

### 2.1. Preparation of MCPB

MCPB consists of powders and cement liquid (water), and the MCPB powders are composed of MgO and calcium dihydrogen phosphate ( $\text{Ca}(\text{H}_2\text{PO}_4)_2 \cdot \text{H}_2\text{O}$ ) in a molar ratio of 2 : 1, which was designed based on an acid–base neutralization reaction as follows:



The MgO was prepared by heating magnesium carbonate pentahydrate in a furnace at  $1500^\circ\text{C}$  for 6 h. The resultant powder was cooled to room temperature (RT), and then ground in a planetary ball mill for 3 min, followed by sieving (120 mesh). The biocement paste was formed by mixing MCPB powders with water at different powder/liquid (P/L) mass ratios, and the mixture was stirred for 1 min to form homogeneous pastes. The mixture of MCPB paste was placed into stainless steel moulds (size  $\Phi 12 \times 3$  mm), and the mixture was modelled under a pressure of 2 MPa. After storage in beakers in a constant temperature oven at  $37^\circ\text{C}$  and 100 per cent relative humidity (r.h.) for different time points, the hardened MCPB sample was obtained.

The hardened MCPB sample was characterized by X-ray diffraction (XRD; Rigaku Co., Japan), and Fourier transform-infrared spectroscopy (FT-IR; Magna-IR 550, Nicolet). The TECP/DCEA system CPB as a control was obtained from Shanghai Rebone Biomaterials Ltd, China. In addition,  $\text{Mg}_3(\text{PO}_4)_2$  and

$\text{Ca}_3(\text{PO}_4)_2$  cements were separately fabricated as controls using two chemical reactions: (i)  $\text{MgO} + \text{H}_3\text{PO}_4$  and (ii)  $\text{CaO} + \text{H}_3\text{PO}_4$ . The surface morphology/microstructure of hardened MCPB (CPB,  $\text{Mg}_3(\text{PO}_4)_2$  and  $\text{Ca}_3(\text{PO}_4)_2$  cements as controls) samples was examined by SEM (JSM-6360LV, JEOL). Except for the setting time and the compressive strength test, the MCPB samples used for other experiments were prepared by setting for 7 days with a P/L mass ratio of  $2.8 \text{ g g}^{-1}$ .

### 2.2. Setting time and compressive strength

The setting time of MCPB (CPB as a control) was determined by a Vicat apparatus bearing a 300 g needle, 1 mm in diameter. The setting time was the number of minutes elapsed from the start of mixing to the time when the needle failed to make a 1 mm deep circle on the surface of the specimen at a temperature of  $37^\circ\text{C}$  and a humidity of 100 per cent. The average value was calculated for each specimen (at least three tests), and the results are expressed as mean  $\pm$  standard deviation (mean  $\pm$  s.d.). Hardened MCPB (CPB as a control) samples for the compressive strength test were obtained by placing the pastes into stainless steel moulds (size  $\Phi 6 \times 10$  mm) at a temperature of  $37^\circ\text{C}$  and 100 per cent humidity for different time points. The compressive strength was measured with a universal testing machine (AG-2000A, Shimadzu) at a speed of  $1 \text{ mm min}^{-1}$  until failure. Three replicates were carried out for each group, and the results are expressed as mean  $\pm$  s.d.

### 2.3. Degradation in Tris–HCl solution

The degradation of MCPB (CPB as a control) in Tris–HCl solution (buffer solution, pH = 7.4) was determined by its weight loss ratio at different time points. The samples ( $\Phi 12 \times 3$  mm) were immersed in Tris–HCl solution at  $37^\circ\text{C}$  and a solid/liquid mass ratio of  $0.5 \text{ g g}^{-1}$ ; the solution was refreshed every 3 days. After soaking, the specimens were removed from the liquid, rinsed with distilled water and dried in an oven for 2 h. All the values reported are averages of three specimens. The percentage of weight loss was computed as follows:

$$\text{Weight loss (\%)} = \frac{(W_0 - W_t)}{W_0} \times 100,$$

where  $W_0$  is the starting dry weight and  $W_t$  is the dry weight at time  $t$ . Furthermore, the surface morphology/microstructure of MCPB samples after immersing in Tris–HCl for 30 days was characterized by SEM. MCPB samples were incubated in Tris–HCl solution for 3 days without changing the solution, and changes in the concentration of Ca, Mg and P ions in the Tris–HCl solution were monitored by inductively coupled plasma-atomic emission spectroscopy (ICP-AES) at 1, 6, 12, 24, 48 and 72 h. The pH of the Tris–HCl solution after soaking in MCPB was measured using an electrolyte-type pH meter for 7 days without changing the solution.

#### 2.4. Cell proliferation

To evaluate the cellular proliferation on the MCPB, the hardened MCPB samples ( $\Phi$  12  $\times$  3 mm) were sonicated in ethanol and sterilized using an autoclave at 120°C for 30 min; CPB and tissue-cultured polystyrene (TCP) were used as controls. The MCPB samples were then seeded with MG<sub>63</sub> cells at a density of  $1 \times 10^5$  cells per sample, and incubated at 37°C and 100 per cent humidity with 5 per cent CO<sub>2</sub> in Dulbecco's modified essential medium (DMEM) 10 per cent foetal calf serum (FCS) medium for 1, 3 and 5 days, and the medium was replaced every 2 days. Cell viability was quantified using 3-(4,5-dimethylthiazol-2-yl)-2,5-diphenyltetrazolium bromide (MTT) assay. In brief, the cells per sample constructs were placed in a culture medium containing MTT, which was incubated in a humidified atmosphere at 37°C for 4 h, and the optical density (o.d.) of the chromophore was measured at 492 nm using an enzyme-linked immunoadsorbent assay plate reader. Six specimens were tested for each incubation period, and each test was performed in triplicate. Results were reported as units of o.d. absorbance value and presented as mean  $\pm$  s.d.

#### 2.5. Cell morphology

To evaluate the effects of MCPB on the morphology and spread of the cultured cells, MG<sub>63</sub> cells were incubated with the MCPB specimens ( $\Phi$  12  $\times$  3 mm) under a humidified atmosphere at 37°C and 5 per cent CO<sub>2</sub>, and the morphology of the cells on the MCPB specimens at 3 and 5 days was observed by SEM. The cells were allowed to attach to the substrates for 24 and 72 h in a humidified atmosphere at 37°C and 5 per cent CO<sub>2</sub>, respectively. At each time point, the MCPB specimens were removed and washed with phosphate-buffered saline (PBS) twice and fixed in 2.5 per cent glutaraldehyde in 0.1 M sodium-PBS for 30 min. The fixed cells were washed with PBS three times, and then dehydrated in ascending concentrations of ethanol (30, 50, 70, 90, 95, 100 (v/v)) for 5 min. The specimens were prepared by first immersing in 50 per cent alcohol-HMDS (hexamethyldisilazane) solution (v/v) for 10 min and then in pure HMDS for 10 min. Later, the samples were vacuum-dried at 37°C overnight, and the cell morphology of the dried specimens was observed using SEM.

#### 2.6. ALP activity

MG<sub>63</sub> cells were seeded on the MCPB ( $\Phi$  12  $\times$  3 mm) at  $5 \times 10^4$  cells per sample, with CPB and tissue-cultured polystyrene (TCP) as controls, and the ALP activity of the cells was measured. At the end of 7 days of incubation, the culture medium in 24-well plates was aspirated. Approximately 200  $\mu$ l of 1 per cent Nonidet P-40 (NP-40) solution was added to each well at RT and incubated for 1 h. The cell lysate was obtained and centrifuged. Exactly 50  $\mu$ l of supernatant was added to 96-well plates; 50  $\mu$ l of 2 mg ml<sup>-1</sup> *p*-nitrophenylphosphate (Sangon, Shanghai, China) substrate solution composed of 0.1 mol l<sup>-1</sup> glycine, 1 mmol l<sup>-1</sup> MgCl<sub>2</sub>·6H<sub>2</sub>O was added and incubated for 30 min at 37°C. The reaction was quenched by adding 100  $\mu$ l of

0.1 N NaOH, and the absorbance of ALP was quantified at a wavelength of 405 nm using a microplate reader (SPECTRAMax 384, Molecular Devices, USA). The total protein content in the cell lysate was determined using the bicinchoninic acid method in aliquots of the same samples with the Pierce protein assay kit (Pierce Biotechnology Inc., Rockford, IL, USA), read at 565 nm and calculated according to a series of albumin (bovine serum albumin) standards. The ALP levels were normalized to the total protein content, and all the experiments were performed in quadruplicate.

#### 2.7. Statistical analysis

Statistical analysis was performed using Student's *t*-test. The results are presented as mean  $\pm$  s.d. (mean  $\pm$  s.d.). Differences are considered statistically significant at  $p < 0.05$ .

### 3. RESULTS

#### 3.1. Setting time

The effect of P/L mass ratio on the setting time of MCPB is shown in figure 1*a*. The setting time of MCPB increased with an increase in the P/L ratio. When the P/L ratio was more than 5 g g<sup>-1</sup>, the mixture of MCPB powder and liquid was too dry to mix and could not form a cement paste. On the other hand, when the P/L ratio was less than 1.9 g g<sup>-1</sup>, the mixture of cement powder and solution was too thin to handle and also could not form cement dough (difficult to harden). The hardening mechanisms in this study had some similarity to the previous study (Xu & Simon 2005). When the P/L ratio was 3.6, 2.8 and 2.3 g g<sup>-1</sup>, the corresponding setting times were 6, 7 and 10 min. In view of the compressive strength (shown in figure 2), setting time and other factors, we chose a P/L ratio of 2.8 g g<sup>-1</sup> to prepare the cement samples for other experiments. For CPB, when the P/L ratio was 2.8 g g<sup>-1</sup>, the setting time was 16 min. When compared with CPB, MCPB had a shorter setting time, indicating that MCPB had a faster setting property.

#### 3.2. Compressive strength

Figure 1*b* shows the effect of the P/L ratio on the compressive strength of MCPB. The compressive strength increased with an increase in the P/L ratio, and reached a maximum value of 73 MPa after 2 days of setting when the P/L ratio was 0.36 g g<sup>-1</sup>. However, the compressive strength decreased with a further increase in P/L ratio. The results indicate that the change in P/L ratio obviously affected the compressive strength of MCPB. The effect of the hardening time on compressive strength of MCPB is shown in figure 2. It was found that the compressive strength of MCPB changed with time during setting. The initial compressive strength of MCPB reached 43 MPa at 1 h, while CPB reached only 13 MPa; later, the compressive strength of MCPB slightly increased with time. After 7 days of setting, the compressive strength of MCPB reached as high as 74 MPa with a P/L ratio of 2.8 g g<sup>-1</sup>, while the compressive strength of CPB was only 36 MPa.

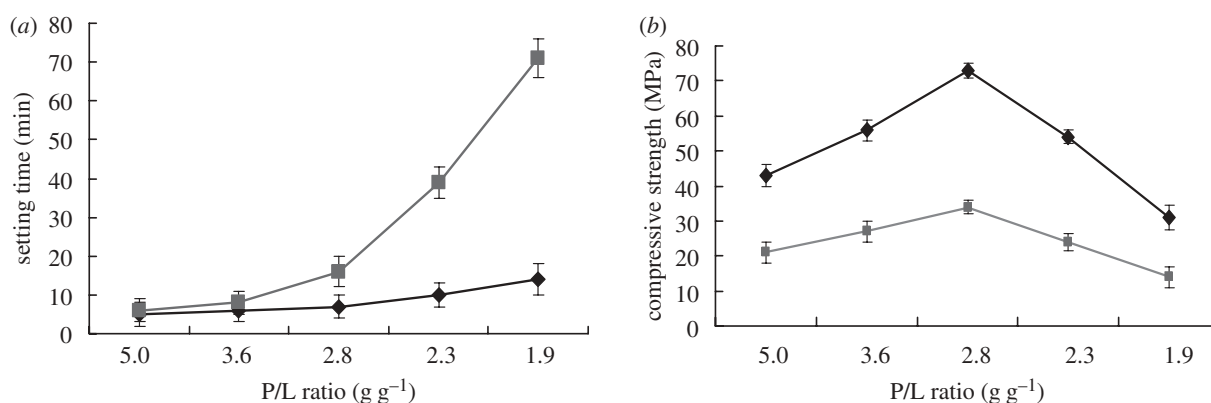


Figure 1. Effect of P/L mass ratio on (a) setting time and (b) compressive strength of MCPB after setting for 48 h. Diamonds, MCPB; squares, CPB.

The results indicate that the compressive strength of MCPB was significantly higher than that of CPB.

### 3.3. XRD and IR analysis

The phase composition of the hardened MCPB was characterized by XRD as shown in figure 3. The MCPB contained a mixture of magnesium phosphate ( $\text{Mg}_3(\text{PO}_4)_2$ ) and calcium phosphate ( $\text{Ca}_3(\text{PO}_4)_2$ ). The presence of magnesium phosphate and calcium phosphate could be attributed to the acid–base neutralized reaction of  $\text{MgO}$  and  $\text{Ca}(\text{H}_2\text{PO}_4)_2 \cdot \text{H}_2\text{O}$ . Figure 4 shows the IR analysis of the hardened MCPB. The absorption bands at 1070.8 and 950  $\text{cm}^{-1}$  were ascribed to  $\text{PO}_4^{3-}$ . The two peaks at 1432.2 and 1750.8  $\text{cm}^{-1}$  and the broad band from 2800 to 3472.2  $\text{cm}^{-1}$  were attributed to the absorbed water. The band at 877.7  $\text{cm}^{-1}$  might correspond to the vibration of P–O–H from  $\text{Mg}_3(\text{PO}_4)_2$  and  $\text{Ca}_3(\text{PO}_4)_2$ . No OH-specific peaks were found at 1571  $\text{cm}^{-1}$  and 631  $\text{cm}^{-1}$ , indicating that no hydroxyapatite appeared in the finally hardened products. The results of the IR analysis were in accordance with the XRD analysis.

### 3.4. SEM analysis

Figure 5 presents SEM images of the surface morphology/microstructure of MCPB after setting for 7 days. It was found that the MCPB contained cylinder-like crystals and clay-like substances to form a dense structure, and the crystals were in close proximity to the clay-like substances as shown in figure 5a. Examination at greater magnifications of MCPB revealed that many cylinder-like crystals with typical  $\text{Mg}_3(\text{PO}_4)_2$  morphology appeared. These well-grown cylinder-like crystals of around 2  $\mu\text{m}$  were embedded into clay-like substances. In addition, the clay-like substance consisted of some small particles of around 100 nm, which might be  $\text{Ca}_3(\text{PO}_4)_2$ , as shown in figure 5b.

In order to create controls,  $\text{Mg}_3(\text{PO}_4)_2$  cement was fabricated using a reaction of  $\text{MgO}$  and  $\text{H}_3\text{PO}_4$ , and  $\text{Ca}_3(\text{PO}_4)_2$  cement was also prepared using a reaction of  $\text{CaO}$  and  $\text{H}_3\text{PO}_4$ . It can be seen that many well-grown cylindrical crystals of  $\text{Mg}_3(\text{PO}_4)_2$  were compactly combined with each other (figure 5c), which was similar

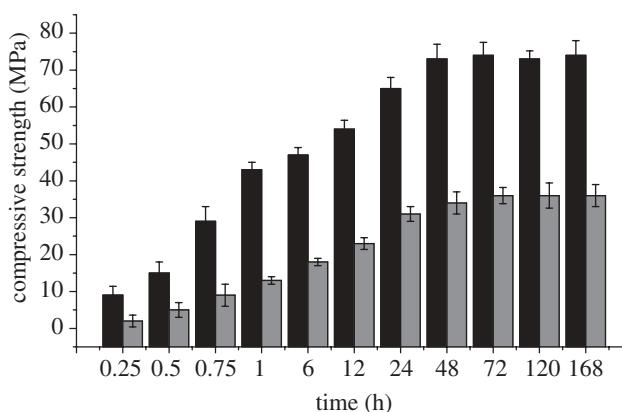


Figure 2. Effect of hardening time on compressive strength of MCPB with a P/L ratio of 2.8  $\text{g g}^{-1}$ . Black bar, MCPB; grey bar, CPB.

to the cylindrical crystals of  $\text{Mg}_3(\text{PO}_4)_2$  shown in figure 5a,b. Furthermore, the morphology of  $\text{Ca}_3(\text{PO}_4)_2$  cement (clay-like substances) (figure 5d) was found to be similar to  $\text{Ca}_3(\text{PO}_4)_2$  (figure 5a,b). The results revealed that the MCPB had changed into a mixture of magnesium phosphate and calcium phosphate by an acid–base neutralized reaction.

### 3.5. Degradation in Tris–HCl solution

Figure 6a presents the weight loss ratio of both MCPB and CPB samples immersed in Tris–HCl solution versus time. Clearly, both MCPB and CPB samples degraded in Tris–HCl solution with time, and the weight loss ratio reached 84.23 and 9.67 wt% for MCPB and CPB at 90 days, respectively. The results showed that the degradation of MCPB was significantly faster than that of CPB. Figure 6b,c shows the surface morphology/microstructure of MCPB after immersion in Tris–HCl solution for 30 days. Some deep cracks were found on the surface of the MCPB, as shown in figure 6b. In addition, the surface of MCPB was eroded and formed many micropores (figure 6c), which might increase the surface area of MCPB, and accelerate the dissolution process.

Figure 7 shows the change in ion concentrations of Ca, Mg and P in Tris–HCl solutions after soaking MCPB and CPB for various time periods. The ion

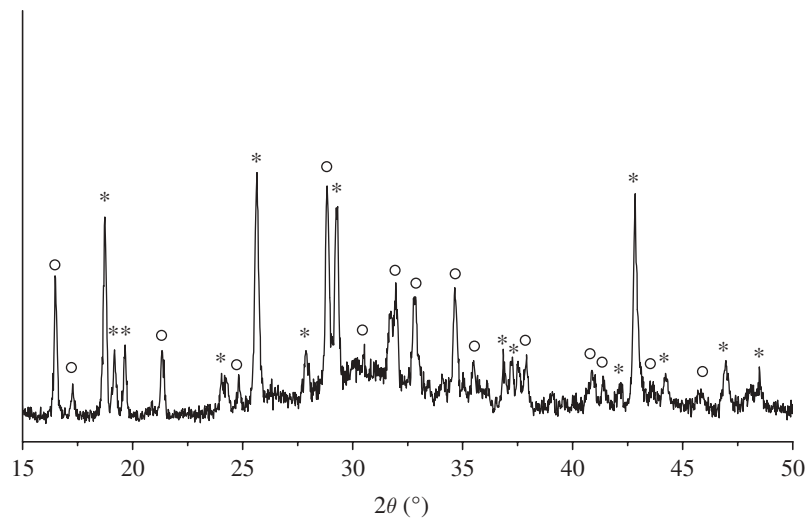


Figure 3. XRD patterns of MCPB after setting for 7 days with a P/L mass ratio of  $2.8 \text{ g g}^{-1}$ . Open circles,  $\text{Ca}_3(\text{PO}_4)_2$ ; asterisks,  $\text{Mg}_3(\text{PO}_4)_2$ .

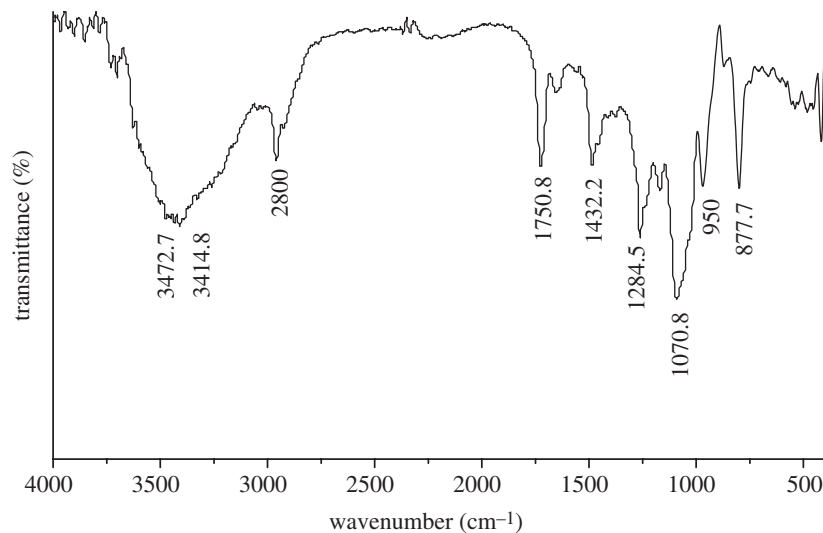


Figure 4. FT-IR spectra of MCPB after setting for 7 days with a P/L mass ratio of  $2.8 \text{ g g}^{-1}$ .

concentration of Ca, Mg and P in Tris–HCl solution increased over time for MCPB within 3 days. In addition, there was a more rapid increase in Ca and P ion concentrations with MCPB than with CPB during soaking. The change in pH value of the Tris–HCl solution after immersion of MCPB and CPB at different time points is shown in figure 8. The results reveal that the pH of the Tris–HCl solution for MCPB decreased from 7.5 to 7.25 within 24 h; thereafter, it increased slightly from 7.25 to 7.3 within the next 168 h. On the other hand, the pH for CPB varied from 7.4 to 7.2 within 168 h. The results show that no obvious difference in pH change between MCPB and CPB was found during soaking.

### 3.6. Cell culture

**3.6.1. Cell proliferation.** The proliferation of  $\text{MG}_{63}$  cells cultured on both MCPB and CPB was assessed using the MTT assay because o.d. values can provide an indicator of the cell growth and proliferation on biomaterials.

It is found from figure 9 that the o.d. value for MCPB was significantly higher than that for CPB at 3 and 5 days ( $p < 0.05$ ); no significant difference was found at 1 day for both MCPB and CPB. The results show that MCPB could promote cell proliferation when compared with CPB and control (TCP), suggesting that MCPB facilitated cell proliferation.

**3.6.2. Cell morphology.** Scanning electron micrographs of  $\text{MG}_{63}$  cells cultured on MCPB for 3 and 5 days are shown in figure 10. After 3 days, the cells had firmly attached and spread well on the MCPB surface, and exhibited normal morphology, as shown in figure 10a. In addition, after 5 days, cells spread well and formed a confluent layer with intimate attachment to the sample surface, as shown in figure 10b. The results indicated that the MCPB had good cytocompatibility with no negative effects on cell morphology and viability.

**3.6.3. ALP activity.** The cellular differentiation was assessed by testing the ALP activity of  $\text{MG}_{63}$  cells

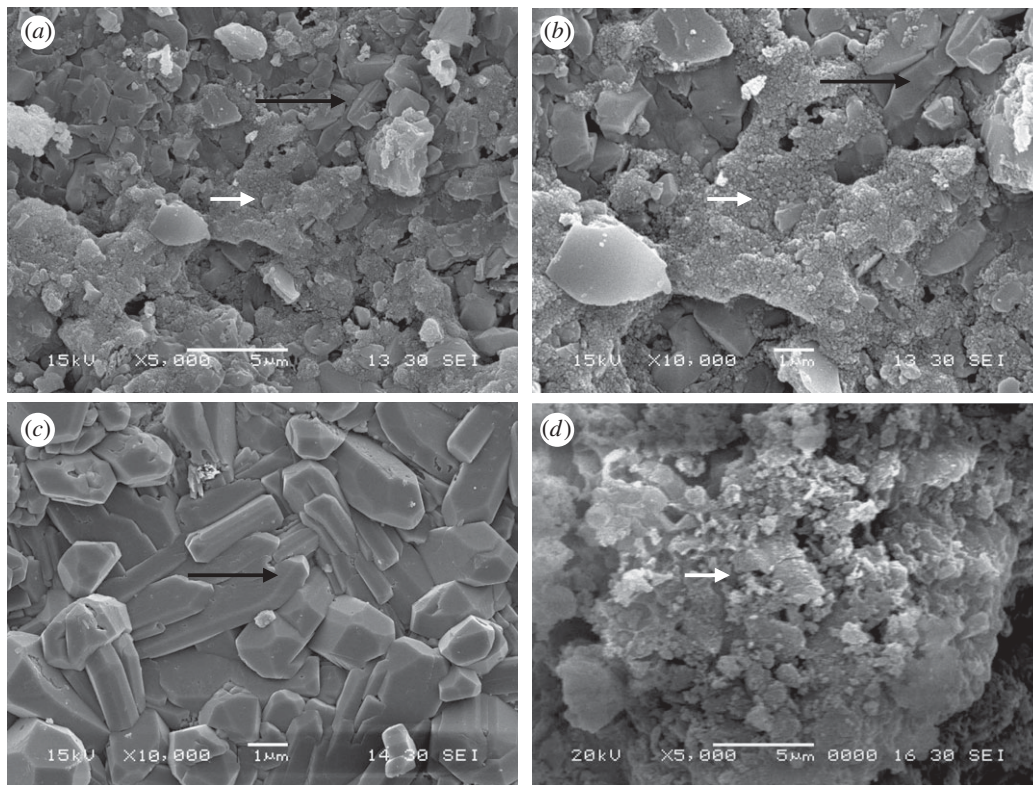


Figure 5. SEM images of the morphology and microstructure of MCPB after setting for 7 days with a P/L mass ratio of  $2.8 \text{ g g}^{-1}$  under different magnifications (*a*,  $5000\times$  and *b*,  $10\,000\times$ ); long arrow represents  $\text{Mg}_3(\text{PO}_4)_2$ ; short arrow represents  $\text{Ca}_3(\text{PO}_4)_2$ .  $\text{Mg}_3(\text{PO}_4)_2$  (*c*,  $10\,000\times$ ) and  $\text{Ca}_3(\text{PO}_4)_2$  (*d*,  $5000\times$ ) as controls.

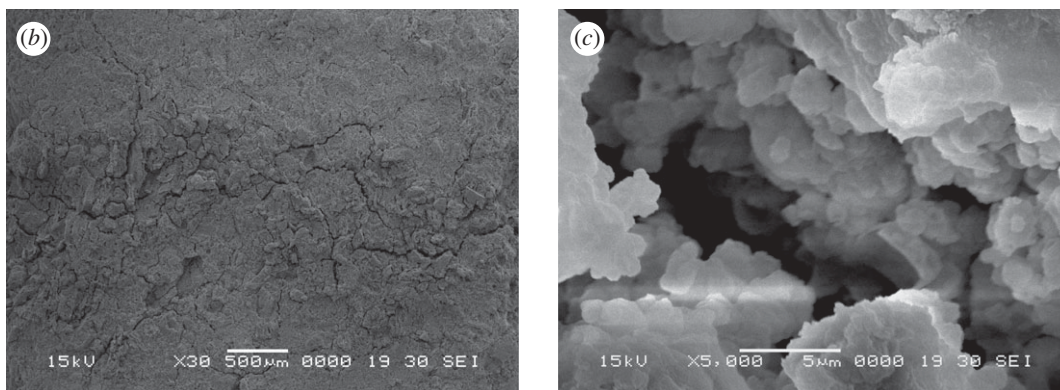
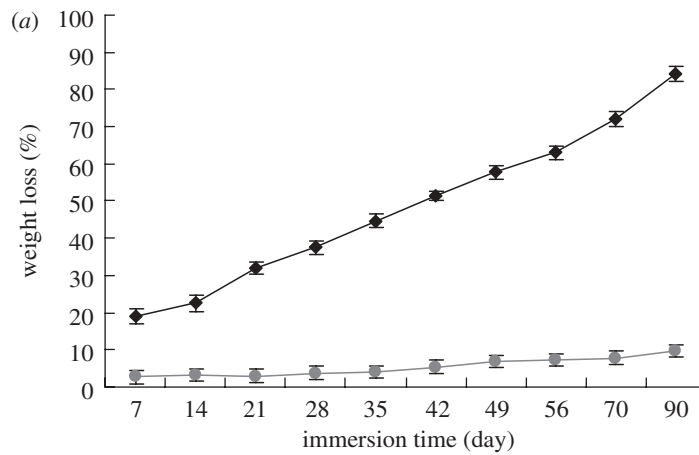


Figure 6. Weight loss ratios of MCPB (CPB as a control) immersed in Tris-HCl solution with time (*a*: diamonds, MCPB; circles, CPB), and SEM images of the morphology/microstructure of MCPB after immersion in Tris-HCl solution for 30 days under different magnifications, (*b*)  $30\times$  and (*c*)  $5000\times$ .

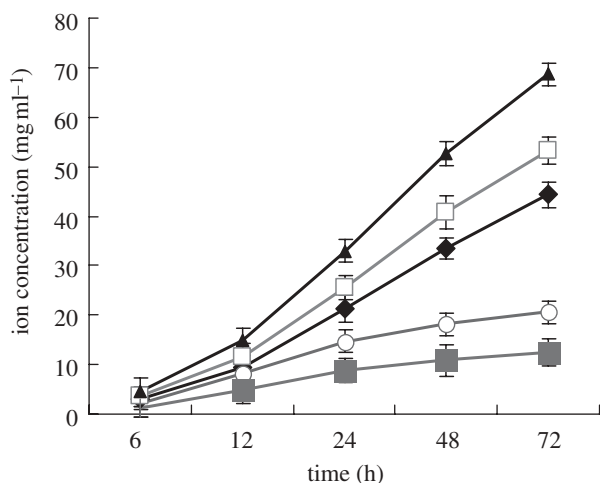


Figure 7. Tendency of Ca, Mg, P ion concentrations to change in Tris–HCl solution after immersion of MCPB and CPB for 3 days. Diamonds, MCPB[Ca]; open squares, MCPB[Mg]; triangles, MCPB[P]; circles, CPB[Ca]; filled squares, CPB[P].

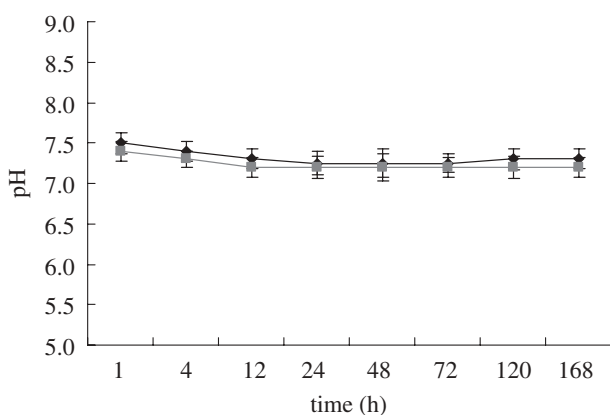


Figure 8. Change in pH of Tris–HCl solution after MCPB and CPB immersion for 7 days. Diamonds, MCPB; squares, CPB.

cultured on MCPB at 4, 7 and 14 days, as shown in figure 11. The ALP activity of MG<sub>63</sub> cells cultured on the MCPB was significantly higher than that of CPB and the control (TCP) at 7 and 14 days ( $p < 0.05$ ). A previous study showed that the ALP for mesenchymal stem cells on CPC–chitosan was higher than on CPC at 14 days (Moreau & Xu 2009). There were no significant differences for ALP at 7 and 14 days for the same sample. Thus, the osteoblasts had differentiated better on the MCPB than on the CPB at 7 and 14 days.

#### 4. DISCUSSION

Rapid setting and high initial mechanical strength of MCPB was designed and fabricated by using a mixture of  $\text{Ca}(\text{H}_2\text{PO}_4)_2 \cdot \text{H}_2\text{O}$  and MgO as cement powders. The MCPB powders mixed with cement liquid (water) could be easily handled as a paste and they harden within about 7 min. The hydrated reaction of the cement is a complicated process that is affected by many factors, in which the P/L mass ratio plays an important role in the characteristics of the cements, such as setting

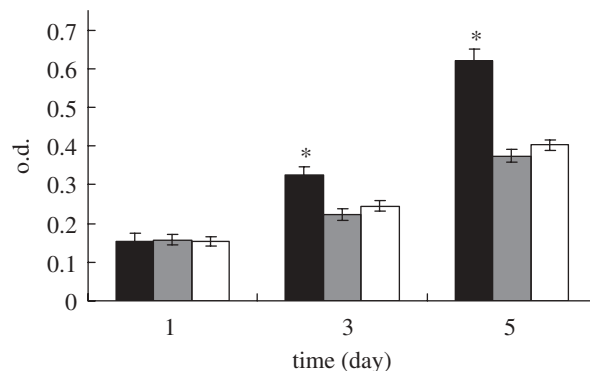


Figure 9. Cell proliferation on MCPB, CPB and control (TCP) at 1, 3 and 5 days. Black bar, MCPB; grey bar, CPB; unfilled bars, control.  $*p < 0.05$ .

time and mechanical strength (Guo *et al.* 2009). In this study, the results showed that the setting time of MCPB increased with an increase in the P/L ratio. When the P/L ratio was  $2.8 \text{ g g}^{-1}$ , setting time was 7 min, indicating that MCPB set faster than CPB, which had a setting time of 16 min. Fast setting is desirable because a long setting time can result in crumbling of the inserted paste if it comes into early contact with physiological fluids, or when bleeding occurs because of the difficulty of achieving complete haemostasis in some cases (Xu *et al.* 2004).

To be suitable for use in bone defect repair, a bone cement should not only have the characteristics of rapid setting but also adequate stiffness, which confers immediate load-bearing capacity and stiffness resembling the natural bone more closely (Li *et al.* 2000; Burguera *et al.* 2006). Moreover, high early strength is needed to prevent early-stage implant failure or disintegration (Dorozhkin 2008). In this study, the initial compressive strength of MCPB reached 43 MPa after setting for 1 h. After 7 days of setting, the compressive strength of MCPB reached as high as 74 MPa. The results suggested that the MCPB with good mechanical properties might be used for load-bearing bone repair in some situations besides being a filler for bone cavity. Besides the setting time, the P/L mass ratio also affects the compressive strength of the cements. Our results showed that the compressive strength of the MCPB increased with an increase in the P/L ratio, and a maximum value of 73 MPa was reached after setting for 48 h with the P/L ratio of  $2.8 \text{ g g}^{-1}$ . However, the compressive strength decreased with a further increase of P/L ratio because of more cement liquid (water) in the paste, which caused higher porosity in the hardened cement.

The hardened MCPB consisted of a mixture of magnesium phosphate ( $\text{Mg}_3(\text{PO}_4)_2$ ) and calcium phosphate ( $\text{Ca}_3(\text{PO}_4)_2$ ), as demonstrated by XRD, IR and SEM. The presence of magnesium phosphate and calcium phosphate could be attributed to the acid–base neutralized reaction of MgO and calcium dihydrogen phosphate. When using MgO and  $\text{Ca}(\text{H}_2\text{PO}_4)_2 \cdot \text{H}_2\text{O}$  in a molar ratio of 2:1, the final hardened product from the acid–base neutralization reaction was  $\text{Mg}_3(\text{PO}_4)_2$  and  $\text{Ca}_3(\text{PO}_4)_2$ , which was in accordance with our

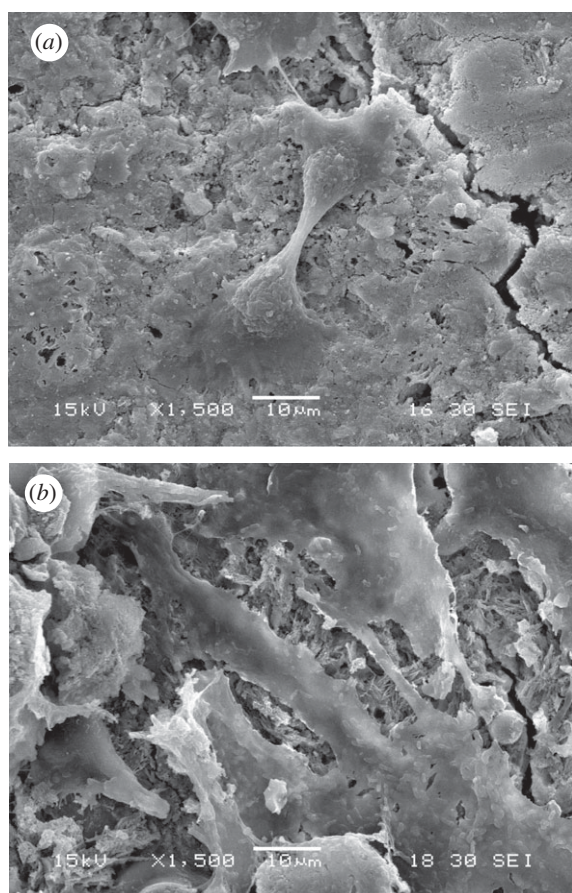


Figure 10. SEM images of MG<sub>63</sub> cells cultured on MCPB for (a) 3 and (b) 5 days.

theoretical design. The SEM images showed that the Mg<sub>3</sub>(PO<sub>4</sub>)<sub>2</sub> appeared to be cylinder-like crystals and Ca<sub>3</sub>(PO<sub>4</sub>)<sub>2</sub> formed clay-like substances in the morphology/microstructure of MCPB. The well-grown cylindrical crystals with typical Mg<sub>3</sub>(PO<sub>4</sub>)<sub>2</sub> morphology dispersed into MCPB and were embedded by the clay-like substances of Ca<sub>3</sub>(PO<sub>4</sub>)<sub>2</sub>; this might enhance the mechanical properties of MCPB (like grain-reinforced cement).

It is accepted that the biomaterials used for bone regeneration should be degradable and gradually replaced by newly formed bone tissue (Hench & Polak 2002). However, previous studies have shown that degradability of TECP/DCPA-based CPB was very slow both *in vivo* and *in vitro* (Dorozhkin & Epple 2002; Guo *et al.* 2009). In this study, the results revealed that the percentages of weight loss ratio of MCPB and CPB were 84.23 and 9.67 wt% after immersion in Tris–HCl solution for 90 days, respectively, indicating that the degradation of MCPB was significantly faster than that of CPB. The quick degradation of MCPB should be attributed to its rapid dissolution performance. Compared with CPB, the degradation of MCPB was accelerated because of the presence of Mg<sub>3</sub>(PO<sub>4</sub>)<sub>2</sub> and Ca<sub>3</sub>(PO<sub>4</sub>)<sub>2</sub>, which was different from the hydrated product (HA) of CPB that had a relatively low dissolution rate, leading to the slow degradation.

The surface morphology/microstructure of MCPB immersed in Tris–HCl solution after 30 days revealed

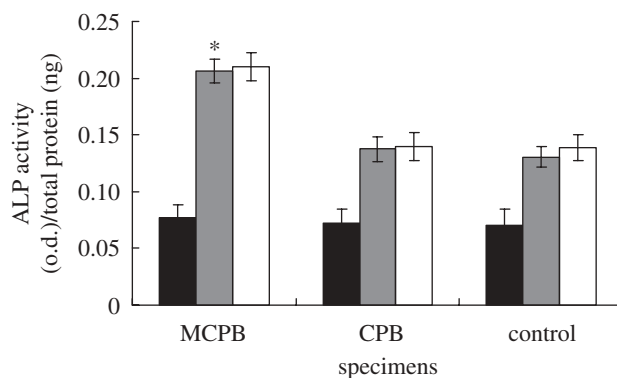


Figure 11. ALP activity of MG<sub>63</sub> cells cultured on the MCPB, CPB and control (TCP) at 4 (black bars), 7 (grey bars) and 14 (unfilled bars) days. \**p* < 0.05.

that some deep cracks were found on its surface, and as the surface of MCPB was eroded and many micropores were formed, this might accelerate the degradation process. In addition, the ion concentrations of Ca, Mg and phosphate increased with time in Tris–HCl solution, indicating that the degradation of MCPB was because of the dissolution of Ca, Mg and phosphate ions from this material into the solution. Moreover, the pH of the Tris–HCl solution slightly decreased from 7.5 to 7.3 up to 168 h. The final pH value was nearly 7.3, which was very suitable for the cell growth (Bodde *et al.* 2008).

Ideally, bioactive biomaterials need to interact actively with cells and stimulate cell growth (Saboori *et al.* 2009; Sader *et al.* 2009). Experiments of cell culture were carried out to test the cytocompatibility of MCPB in this study. The MG<sub>63</sub> cells could proliferate on the MCPB, as demonstrated by the MTT assay, suggesting positive cellular responses to this material. Furthermore, the proliferation rate was obviously enhanced on the MCPB when compared with the CPB, indicating that the MCPB could promote cellular proliferation more effectively than CPB. Thus, the MCPB was cytocompatible, with no obvious negative effects on cellular viability or proliferation. Besides proliferation, the ability of the cells to differentiate on the biomaterials also indicates cell viability and indirectly shows that the materials are biocompatible (Ni *et al.* 2008). ALP activity has been used as an early marker for functionality and differentiation of osteoblasts during *in vitro* experiments (Benoit *et al.* 2008). Our results showed that the ALP activity of the cells on the MCPB exhibited significantly higher levels of expression than those on CPB at 7 and 14 days, indicating that the MCPB facilitated cell differentiation.

Previous studies have reported that ion-dissolution products containing Ca and Mg from bioactive glasses and ceramics could stimulate cell proliferation (Dietrich *et al.* 2009; Sader *et al.* 2009). It is believed that the release of Mg ions from corroding Mg alloys should not cause toxicity (local or systemic), and may even have beneficial effects on cell responses, in the relevant local tissue (Staiger *et al.* 2006; Witte *et al.* 2007). In this study, the Mg and Ca ions were released from the MCPB into the Tris–HCl solution, and the MCPB resulted in a more rapid increase in Ca and Mg ion



concentrations than CPB, providing higher Ca and Mg ion concentrations in the Tris–HCl solution. Moreover, the MTT assay revealed that MCPB had significantly stimulated MG<sub>63</sub> cell proliferation compared with CPB over time, and ALP tests showed that the MCPB exhibited significantly increased cell differentiation compared with CPB. This probably resulted from the release of Mg and Ca ions from MCPB into the cell culture medium. The continuous dissolution associated with the MCPB produced a Ca- and Mg-rich environment that might be responsible for stimulating cell proliferation and differentiation.

The biocompatibility and bioactivity of biomaterials is very closely related to the cell behaviour in contact with them and particularly to the cell spread on their surface (Otsuka *et al.* 2008). SEM results showed that the cells spread well and formed a confluent layer with very close attachment to the sample surface, while maintaining physical contact with each other. These results indicate that the MCPB had no negative effects on cell morphology and viability. In short, the reason for the excellent cell responses to MCPB mentioned above might be the local chemical environment, in which the MCPB released Mg and Ca ions. In addition, the process of cell spread on the material's surface was influenced by the underlying substrates (Lee *et al.* 2008; Trimbach *et al.* 2008). Our results suggest that the MCPB had a good bioactive surface that was favourable for cell adhesion and growth, which implied good biocompatibility.

## 5. CONCLUSIONS

MCPB with rapid-setting and degradable characteristics was developed by using a mixture of calcium dihydrogen phosphate and MgO as cement powders. The MCPB could be easily handled as a paste that could harden within about 7 min, and achieved a compressive strength of 43 MPa after setting for 1 h, indicating that the rapid-setting MCPB had high initial mechanical strength. After the acid–base hydrated reaction of MgO and Ca(H<sub>2</sub>PO<sub>4</sub>)<sub>2</sub>·H<sub>2</sub>O in a molar ratio of 2 : 1, the final hardened products consisted of Mg<sub>3</sub>(PO<sub>4</sub>)<sub>2</sub> and Ca<sub>3</sub>(PO<sub>4</sub>)<sub>2</sub>. The MCPB was degradable in Tris–HCl solutions because of its rapid dissolution, and the degradation was significantly faster than CPB. The growth and proliferation of MG<sub>63</sub> cells on MCPB were significantly enhanced when compared with CPB, revealing excellent biocompatibility. The ALP activity of MG<sub>63</sub> cells expressed obviously higher levels on MCPB than on CPB at 7 and 14 days, revealing that the MCPB facilitated cell differentiation. The MG<sub>63</sub> cells attached and spread well onto the MCPB substrate with close contact with its surface, showing good cytocompatibility. In conclusion, the results suggest that MCPB shows promise in its development as a bioactive biomaterial for bone regeneration.

The authors appreciate financial support from the National Natural Science Funds of China (no. 30970720), Nano special programme of Science and Technology Development of Shanghai (no. 0852nm02700), Standard Special programme of Science and Technology Development of

Shanghai (no. 08DZ0501600), Major Programme of National Natural Science Foundation of China (no. 50732002), Programme for Changjiang Scholars and Innovative Research Team in University, and Sponsored by Shanghai Pujiang Programme (2008).

## REFERENCES

- Arise, R. O., Davies, F. F. & Malomo, S. O. 2008 Independent and interactive effect of Mg<sup>2+</sup> and Co<sup>2+</sup> on some kinetic parameters of rat kidney alkaline phosphatase. *Sci. Res. Ess.* **3**, 488–494.
- Benoit, D. S. W., Schwartz, M. P., Durney, A. R. & Anseth, K. S. 2008 Small functional groups for controlled differentiation of hydrogel-encapsulated human mesenchymal stem cells. *Nat. Mater.* **7**, 816–823. (doi:10.1038/nmat2269)
- Bodde, E. W. H., Boerman, O. C., Russel, F. G. M., Mikos, A. G., Spauwen, P. H. M. & Jansen, J. A. 2008 The kinetic and biological activity of different loaded rhBMP-2 calcium phosphate bio cement implants in rats. *J. Biomed. Mater. Res. A* **87**, 780–791.
- Brown, W. E. & Chow, L. C. 1986 A new calcium phosphate water setting bio cement. In *Biocements research progress* (ed. P. W. Brown), pp. 352–379. Westerville, OH: American Ceramic Society.
- Burguera, E. F., Xu, H. H. K. & Weir, M. D. 2006 Injectable and rapid-setting calcium phosphate bone cement with dicalcium phosphate dehydrate. *J. Biomed. Mater. Res. B* **77**, 126–134.
- Cancedda, R., Giannoni, P. & Mastrogiacomo, M. 2007 A tissue engineering approach to bone repair in large animal models and in clinical practice. *Biomaterials* **28**, 4240–4250. (doi:10.1016/j.biomaterials.2007.06.023)
- Dietrich, E., Oudadesse, H., Lucas-Girot, A. & Mami, M. 2009 *In vitro* bioactivity of melt-derived glass 46S6 doped with magnesium. *J. Biomed. Mater. Res. A* **88**, 1087–1096. (doi:10.1002/jbm.a.31901)
- Dorozhkin, S. V. 2008 Calcium orthophosphate cements for biomedical application. *J. Mater. Sci.* **43**, 3028–3057. (doi:10.1007/s10853-008-2527-z)
- Dorozhkin, S. V. & Epple, M. 2002 Biological and medical significance of calcium phosphates. *Angew Chem. Int. Ed.* **41**, 3130–3146. (doi:10.1002/1521-3773(20020902)41:17<3130::AID-ANIE3130>3.0.CO;2-1)
- Gu, X. N., Zheng, Y. F., Cheng, Y., Zhong, S. P. & Xi, T. F. 2009 *In vitro* corrosion and biocompatibility of binary magnesium alloys. *Biomaterials* **30**, 484–498. (doi:10.1016/j.biomaterials.2008.10.021)
- Guo, D. G., Xu, K. W., Sun, H. L. & Yong, H. 2006 Physicochemical properties of TTCP/DCPA system cement formed in physiological saline solution and its cytotoxicity. *J. Biomed. Mater. Res. A* **77**, 313–323.
- Guo, H., Su, J. C., Wei, J., Kong, H. & Liu, C. S. 2009 Biocompatibility and osteogenicity of degradable Ca-deficient hydroxyapatite scaffolds from calcium phosphate cement for bone tissue engineering. *Acta Biomater.* **5**, 268–278. (doi:10.1016/j.actbio.2008.07.018)
- Hench, L. L. & Polak, J. M. 2002 Third-generation biomedical materials. *Science* **295**, 1014–1017. (doi:10.1126/science.1067404)
- Hofmann, M. P., Mohammed, A. R., Perrie, Y., Gbureck, U. & Barralet, J. E. 2009 High-strength resorbable brushite bone cement with controlled drug-releasing capabilities. *Acta Biomater.* **5**, 43–49. (doi:10.1016/j.actbio.2008.08.005)
- Huan, Z. G. & Chang, J. 2007 Self-setting properties and *in vitro* bioactivity of calcium sulfate hemihydrate-tricalcium

- silicate composite bone biocements. *Acta Biomater.* **3**, 952–960. (doi:10.1016/j.actbio.2007.05.003)
- Lee, J. Y., Kang, B. S., Hicks, B., Chancellor, T. F., Chu, B. H., Wang, H. T., Keselowsky, B. J., Ren, F. & Lele, T. P. 2008 The control of cell adhesion and viability by zinc oxide nanorods. *Biomaterials* **29**, 3743–3749. (doi:10.1016/j.biomaterials.2008.05.029)
- Li, Y. W., Leong, J. C. Y., Lu, W. W., Luk, K. D. K., Cheung, K. M. C., Chiu, K. Y. & Chow, S. P. 2000 A novel injectable bioactive bone cement for spinal surgery: a developmental and preclinical study. *J. Biomed. Mater. Res.* **52**, 164–170. (doi:10.1002/1097-4636(200010)52:1<164::AID-JBM21>3.0.CO;2-R)
- Liu, C. S. 1999 *Inorganic bone adhesion agent and its use in human hard tissue repair*. US Patent No. 7094286B2.
- Liu, C. S., Shao, H. F., Chen, F. Y. & Zheng, H. Y. 2006 Rheological properties of concentrated aqueous injectable calcium phosphate biocement slurry. *Biomaterials* **27**, 5003–5013. (doi:10.1016/j.biomaterials.2006.05.043)
- Marchi, J., Dantas, A. C. S., Greil, P., Bressiani, J. C., Bressiani, A. H. A. & Muller, F. A. 2007 Influence of Mg-substitution on the physicochemical properties of calcium phosphate powders. *Mater. Res. Bull.* **42**, 1040–1050. (doi:10.1016/j.materresbull.2006.09.015)
- Moreau, J. L. & Xu, H. H. K. 2009 Mesenchymal stem cell proliferation and differentiation on an injectable calcium phosphate-chitosan composite scaffold. *Biomaterials* **30**, 2675–2682. (doi:10.1016/j.biomaterials.2009.01.022)
- Ni, S. Y., Chang, J. & Chou, L. 2008 *In vitro* studies of novel CaO-SiO<sub>2</sub>-MgO system composite bioceramics. *J. Mater. Sci. Mater. Med.* **19**, 359–367. (doi:10.1007/s10856-007-3186-3)
- Otsuka, M., Oshinbe, A., Legeros, R. Z., Tokudome, Y., Ito, A., Otsuka, K. & Higuchi, W. I. 2008 Efficacy of the injectable calcium phosphate ceramics suspensions containing magnesium, zinc and fluoride on the bone mineral deficiency in ovariectomized rats. *J. Pharm. Sci.* **97**, 421–432. (doi:10.1002/jps.21131)
- Revell, P. A., Damien, E., Zhang, X. S., Evnas, P. & Howlett, C. R. 2004 The effect of magnesium ions on bone bonding to hydroxyapatite coating on titanium alloy implants. *Bioceramics* **254**, 447–450.
- Rude, R. K. & Gruber, H. E. 2004 Magnesium deficiency and osteoporosis: animal and human observations. *J. Nutr. Biochem.* **15**, 710–716. (doi:10.1016/j.jnutbio.2004.08.001)
- Saboori, A., Rabiee, M., Mutarzadeh, F., Sheikhi, M., Tahriri, M. & Karimi, M. 2009 Synthesis, characterization and *in vitro* bioactivity of sol-gel-derived SiO<sub>2</sub>-CaO-P<sub>2</sub>O<sub>5</sub>-MgO bioglass. *Mater. Sci.* **29**, 335–340.
- Sader, M. S., LeGeros, R. Z. & Soares, G. A. 2009 Human osteoblasts adhesion and proliferation on magnesium-substituted tricalcium phosphate dense tablets. *J. Mater. Sci. Mater. Med.* **20**, 521–527. (doi:10.1007/s10856-008-3610-3)
- Staiger, M. P., Pietak, A. M., Huadmai, J. & Dias, G. 2006 Magnesium and its alloys as orthopedic biomaterials: a review. *Biomaterials* **27**, 1728–1734. (doi:10.1016/j.biomaterials.2005.10.003)
- Trimbach, D. C., Keller, B., Bhat, R., Zankovych, S., Pohlmann, R., Schroter, S., Bossert, J. & Jandt, K. D. 2008 Enhanced osteoblast adhesion to epoxide-functionalized surfaces. *Adv. Funct. Mater.* **18**, 1723–1731. (doi:10.1002/adfm.200701491)
- Witte, F., Feyerabend, F., Maier, P., Fischer, J., Stormer, M., Blawert, C., Dietzel, W. & Hort, N. 2007 Biodegradable magnesium-hydroxyapatite metal matrix composites. *Biomaterials* **28**, 2163–2174. (doi:10.1016/j.biomaterials.2006.12.027)
- Wu, Z. Z., Zhang, J., Chen, T. Y., Liu, C. S. & Chen, Z. W. 2005 Experimental study of a new type of cement on tibia plateau fractures treatment. *Clin. Med. J. China* **12**, 261–264.
- Wu, F., Su, J., Wei, J., Guo, H. & Liu, C. 2008a Injectable bioactive calcium-magnesium phosphate cement for bone regeneration. *Biomed. Mater.* **3**, 1–7. (doi:10.1088/1748-6041/3/4/044105)
- Wu, F., Su, J., Wei, J., Guo, H. & Liu, C. 2008b Self-setting bioactive calcium-magnesium phosphate cement with high strength and degradability for bone regeneration. *Acta Biomater.* **6**, 1873–1884. (doi:10.1016/j.actbio.2008.06.020)
- Xu, H. H. K. & Simon, C. G. 2005 Fast setting calcium phosphate-chitosan scaffold: mechanical properties and biocompatibility. *Biomaterials* **26**, 1337–1348. (doi:10.1016/j.biomaterials.2004.04.043)
- Xu, H. H. K., Takagi, S., Quinn, J. B. & Chow, L. C. 2004 Fast-setting calcium phosphate scaffolds with tailored macropore formation rates for bone regeneration. *J. Biomed. Mater. Res. A* **68**, 725–734. (doi:10.1002/jbm.a.20093)
- Zreiqat, H., Howlett, C. R., Zannettino, A., Evans, P., Schulze-Tanzil, G., Knabe, C. & Shakibaei, M. 2002 Mechanisms of magnesium-stimulated adhesion of osteoblastic cell to commonly used orthopaedic implants. *J. Biomed. Mater. Res.* **62**, 175–184. (doi:10.1002/jbm.10270)